Translated from *Uspekhi Khimii*, 52 1514-1537 (1983) U.D.C. 538.08 + 538.1 + 541.1 + 541.14 + 541.15

Electron Spin Echo Study of the Steric Characteristics of the Formation and Reactions of Radicals in a Solid Phase

Yu.D.Tsvetkov

The general characteristics of electron spin echo (ESE) spectrometers are considered. A Soviet spectrometer and certain foreign instruments used in physicochemical research are described. The fundamental postulates and results of the theory of magnetic dipole-dipole interactions are briefly formulated in relation to the analysis of the results obtained by the ESE method.
Studies by the ESE method of the steric characteristics of chemical reactions in solids are surveyed. Investigations of the structures of radical tracks in irradiated organic and inorganic systems are considered and it is shown that data concerning the pair distribution function with respect to distances in ion—radical pairs can be obtained by the relaxation probe method and the method of double electron—electron resonance in ESE spectroscopy. The principal results of the investigation of the pair distribution in the formation of radicals under the influence of ultraviolet light and γ-rays as well as the changes in the pair distribution in the course of diffusion and reactions of free radicals and atoms in frozen glasses are discussed.
The bibliography includes 64 references.

CONTENTS

I. Introduction 866
II. Electron spin echo spectrometers 867
III. Magnetic dipole—dipole interactions in ESE spectroscopy 869
IV. Radical tracks 871
V. The relaxation probe. Investigation of the distribution with respect to distances in the radical-ion pairs 873
VI. The double electron—electron resonance method in ESE spectroscopy and its applications 877

I. INTRODUCTION

The development of UHF techniques in recent years makes pulsed EPR methods increasingly available for various physicochemical applications. Among these procedures, the electron spin echo (ESE) method—a special pulse variant of EPR, analogous in its experimental formulation to pulsed echo methods in NMR spectroscopy[1,2]—has developed extensively. In this method, under $\omega_0 = \gamma H_0$ resonance conditions (γ is the gyromagnetic ratio for the electron and H_0 the external magnetic field), the spin system is acted upon by a series of UHF pulses and the spontaneous emission from the system—the spin echo signal—is investigated (Fig.1). In the two-pulse variant of the excitation, the primary echo is produced, while in the three-pulse variant a stimulated echo is produced. The first 90° UHF pulse gives rise to a coherent state of the spin system, which is correlated as regards initial phase. The break up of this state into individual "isochromatic components" in the $xy \perp \mathbf{H}_0$ plane of the coordinate system, rotating at a frequency ω_0 about the z axis, is caused by phase relaxation (transverse) processes (with a time T_2) and the restoration of the magnetisation to the equilibrium value M_0 along the $z \parallel \mathbf{H}_0$ axis is due to the spin-lattice relaxation (longitudinal) with a characteristic time T_1. A 180° pulse applied at a time interval τ reverses the movement of the isochromatic component, which gives rise to the echo signal at time 2τ. The signal amplitude $V(2\tau)$ diminishes as the time interval τ between the UHF pulses is altered.

The spin echo for paramagnetic species was first observed by Blume[3,4] (USA) in a study of solutions of sodium in liquid ammonia. The ESE theory has been at present developed in fair detail[5-7]. For physicochemical applications, the following characteristics of the ESE method must be noted.

1. Compared with the stationary EPR method, which constitutes a frequency domain spectroscopy, ESE is a time domain spectroscopy in which the times of the evolution of the spin system (T_1, T_2) are recorded directly.

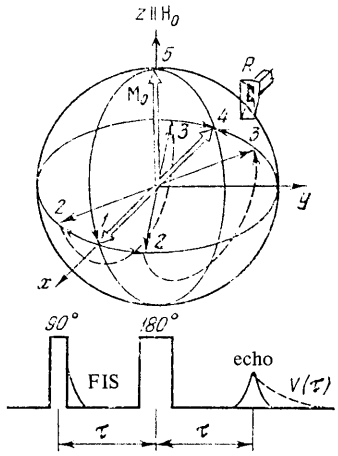


Figure 1. The vector model of the generation of a spin echo signal; a 90° pulse rotates the magnetisation vector $\mathbf{M}_0$ in the xy plane (*1*); decomposition of $\mathbf{M}_0$ into isochromatic components at a rate T_2^{-1} (*2*) inducing a free induction signal (FIS) in the receiver (R); rotation of the isochromatic components by an 180° pulse (*3*); restoration of $\mathbf{M}_0$ along the x direction (*4*)—the generation of the echo signal; restoration of $\mathbf{M}_0$ along the z direction as a result of the spin–lattice relaxation at a rate T_1^{-1}; τ—time between pulses; $V(\tau)$—decay of the echo signal as τ is altered.

2. The possibility of obtaining the ESE signal (the break up of the overall magnetisation vector $\mathbf{M}_0$ into isochromatic components and its subsequent restoration) arises via a mechanism involving the static inhomogeneous broadening of the EPR line, while the kinetics of the decrease of the LSE

signal $V(2\tau)$ with increase of the time interval between the UHF pulses, i.e. the form of the relation, contain information about the different time-dependent stochastic processes in the spin system. These processes also arise as a consequence of magnetic interactions such as magnetic dipolar (electron–electron and electron–nucleus) or exchange interactions. Thus ESE makes it possible to investigate magnetic interactions under conditions uncomplicated by the inhomogeneous static line broadening of the kind which occurs in the stationary EPR.

3. The magnetic interactions in the spin system lead in addition to the modulation of the relaxation decay of the ESE signal. The Fourier transformation of the modulated decrease yields the frequencies and amplitudes of the magnetic interactions. A unique feature of ESE is the possibility of analysing relatively weak hyperfine and quadrupole interactions in polyoriented systems, which creates a basis for structural applications of the method.

4. As a pulsed variant of EPR spectroscopy, ESE can be conveniently combined with various physical and specially pulsed influences on the test system. There exist kinetic variants of ESE in which paramagnetic species are generated by light[8], a laser pulse[9], or a fast electron pulse[10]. Methods in which the system is acted upon by electric field pulses have been developed[11].

In the present review we shall consider only one of the fields of the physicochemical applications of the ESE method—studies of the steric characteristics of the formation and reactions of free radicals, atoms, and ions in solids. These investigations are based on measurements for magnetic dipole–dipole interactions. They were begun at the Institute of Chemical Kinetics and Combustion of the Siberian Division of the USSR Academy of Sciences in 1965 on the initiative of Acad.V.V.Voevodskii. Reviews of the early results may be found in other publications[6,7,12].

II. ELECTRON SPIN ECHO SPECTROMETERS

Approximately 30 ESE spectrometers are actually working or are in the adjustment stage in various laboratories throughout the world. In foreign laboratories the spectrometers are as a rule assembled from separate units purchased from various firms. In contrast to the first models[6,13,14], the instruments constructed nowadays are coherent ESE spectrometers, which implies that, for a fixed phase of the exciting UHF pulses, the phase of the detected ESE signal is also known. A coherent spectrometer is more sensitive than an incoherent one and has a linear characteristic—the change in the amplitude of the detected signal is proportional to the amplitude of the signal applied to the input of the detector. In addition, there is a possibility of direct measurements of the polarisation of the ESE signal, which arises in various chemical reactions, i.e. the phenomenon of the electronic polarisation of the spins[15].

The ESE signal arises when the spin system is acted upon by a series of UHF pulses which rotate the vector $\mathbf{M}_0$ through a definite angle θ. In the two-pulse variant of the excitation, the amplitude of the echo signal is determined by the angles θ_1 and θ_2:

$$V = V(2\tau)\sin\theta_1 \sin^2\frac{\theta_2}{2}$$

$$\theta_{1,2} = \gamma H_1 \tau_{p_{1,2}}$$

where H_1 is the amplitude of the UHF pulse and τ_p its duration. The duration of the pulses in experiments designed to investigate the phase or spin–lattice relaxation must be much shorter than T_1 and T_2. The times T_1, $T_2 \cong 10^{-7}$ s are nowadays of practical interest, so that we must have $\tau_p \cong 2 \times 10^{-8}$ s, which yields $H_1 \cong 5$ G for $\theta = 90°$. Such a strength of the UHF magnetic field is ensured by a source with a pulse power $P_p \cong 1$ kW.[6] Naturally one can employ also less powerful sources for the excitation of the ESE signal. However, one must then bear in mind that, for small H_1, the signal amplitude diminishes in proportion to H_1^3. Furthermore, for a whole series of experiments, including studies of the dipolar interactions and modulation phenomena, one must excite at least a major portion of the EPR spectrum if not the entire spectrum with a width ΔH, i.e. it is necessary that the condition $H_1 \cong \Delta H$ should hold. In general purpose ESE spectrometers the power of the pulses from the exciting source is therefore as a rule ~1 kW.

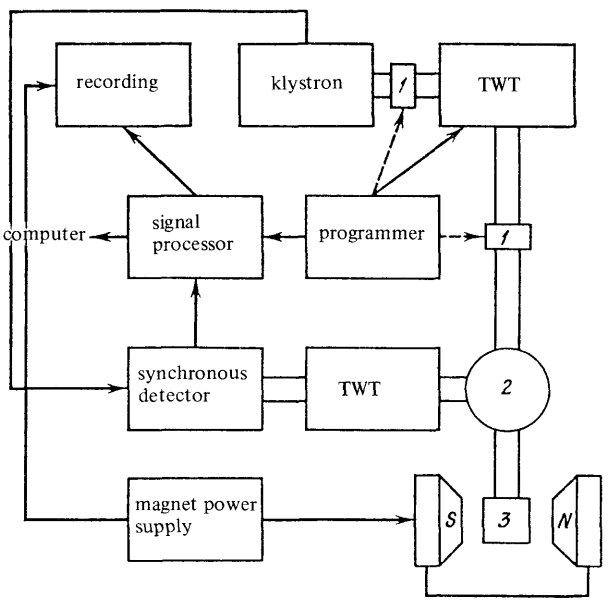


Figure 2. Generalised block schematic of an ESE spectrometer: 1) UHF switch; 2) circulator; 3) cavity; TWT—travelling wave tubes.

A block schematic of a spectrometer for the 3-cm wavelength range is illustrated in a general form in Fig. 2. One or several travelling wave tubes (TWT), which function as amplifiers of the power of the triggering klystron, are usually employed as a source of the UHF pulses; the UHF part of the spectrometer contains standard elements for EPR spectroscopy: attenuators, circulators, phase inverters, and switches. In contrast to EPR spectroscopy, the cavity need not have a high Q factor (see below). Apart from the additional frequency tuning, provision is usually made for reducing the Q factor by introducing an absorbing element such as a carbon or ferrite plate at the antinode of the electric field. Before it reaches the synchronous (balanced) detector, the signal is additionally amplified with the aid of special low-noise and low-inertia TWT. Beyond the detector, the signal in the form of a pulse enters the interpretation unit, which incorporates elements transforming the signal into a digital form, a signal accumulation system, and a system for its treatment in order to suppress noise. In a digital

or analogue form, the signal is applied to the recording device—a pen recorder, a perforated tape, another digital indicator, or a computer.

The most important element of the ESE spectrometer is a programmable pulse sequence generator. By controlling the TWT or UHF switches, it ensures the formation of a train of UHF pulses, determines their duration τ_p, the intervals between the pulses, and the time scan of these intervals as well as the frequency of the repetition of a series of pulses, and controls the signal treatment unit of the recording unit. Finally, each spectrometer contains a scanning unit and a unit for the calibration of the permanent magnetic field H_0.

According to theoretical estimates[6], the sensitivity of the ideal coherent ESE spectrometer is in the range 10^{10}–10^{11} spins in the specimen for a phase relaxation time $T_2 = 3 \times 10^{-7}$ s, a spin–lattice relaxation time $T_1 = 3 \times 10^{-6}$–10^{-4} s, and a signal recording time of 1 s, which corresponds to the sensitivity of modern stationary EPR spectrometers. An increase of sensitivity can be achieved by increasing the recording time as a result of the increased number of accumulations. We may note that, so far as we are aware, measurements of the sensitivity of ESE spectrometers, necessary for comparison with calculated values, are not available in the literature.

For any time domain spectroscopy, the most significant parameter of the ESE spectrometer is its resolving power with respect to time. This parameter should be understood as the minimum relaxation time, for example, the phase relaxation time T_2 recorded by the spectrometer ($T_{2,\min}$). For an ideal spectrometer, on excitation with a train of 90–180° pulses with durations τ_p and $2\tau_p$, we have

$$T_{2,\min}^{id} \geqslant 3\tau_p$$

In the case of a real spectrometer there is in addition a significant contribution by the so-called "ringing" of the cavity. When a resonator is acted upon by pulses, a reflected signal is generated, whose rear front is represented by an exponential function decaying with a time constant $t_0 = Q/2\omega_0$. This signal overloads the UHF amplifier with respect to time[6]:

$$\tau_r = t_0 \ln P_p/pP_n$$

where P_p is the power of the UHF pulse, $P_n = kT\omega_0/2Q$ the power of the noise, and p the amplification factor. Thus the minimum time T_2 which can be recorded by the spectrometer increases by an amount τ_r:

$$T_{2,\min} \geqslant 3\tau_p + \tau_r .$$

For $P_p = 1$ kW, $Q = 500$ $T = 300$, and $p = 100$, this additional so-called "ringing" time or "dead" time of the spectrometer is approximately 120 ns. Taking into account the fact that commuting UHF devices nowadays have a fast response time of ~10–20 ns, the real resolving power of the spectrometer is 200–300 ns. More accurate estimates[5,6] yielded similar values. The simplest method for reducing $T_{2,\min}$, by decreasing Q to low values, is evidently inapplicable because the sensitivity of the spectrometer is proportional to $Q^{1/2}$.[5,6]

The coherent spectrometer of the Institute of Chemical Kinetics and Combustion of the Siberian Division of the USSR Academy of Sciences has been described in full detail in recent literature[16,17]. One of the characteristic features of this apparatus is the possibility of generating UHF pulses with a power up to 5 kW for a minimum duration of 20 ns, which is ensured by a magnetron operating with synthronisation of its frequency and phase by the UHF oscillations of an amplification cascade based on TWT; when only TWT are used, the power of the pulse is 1 kW. Another feature is the modulation of the UHF phase to suppress the signal due to the "ringing" of the cavity and to increase the time resolution. The ESE signal is excited at a specific frequency of the repetition of the "pulse (90°)–pulse (180°)–echo" cycles. If the phase of the first pulse is reversed in each even cycle, then the phase of the echo signal in the even cycles is also rotated by 180° compared with the phase of the signal in odd cycles. The "ringing" signal, which is independent of the phase of the pulses, is the same for even and odd cycles. By subtracting the signals from the even and odd cycles in the signal processor unit, it is possible to suppress the "ringing" signal. The resolving power of such a spectrometer is approximately 2×10^{-7} s.

The programmable pulse sequence generator (programmer) of the spectrometer generates a series of four pulses, one of which is used for external synchronisation and one is a strobe pulse. The duration of the pulses and the intervals between them are regulated in 1 ns steps. These intervals are varied automatically at specified steps and at a specified rate. The programmer also generates a pulse which rotates by 90° the UHF pulse and ensures the time scan of the pen recorder in the spectrometer.

The stability and convenience of the operation of the spectrometer are also ensured by a special device for the stabilisation of the field and its scan by means of an NMR transducer, which makes it possible to determine the field strength to within 3×10^{-4}% and to alter it at a specified rate in the specified range with continuous digital indication of the value of H_0.

A modified variant of the ESE spectrometer described previously[8], was examined briefly in another communication[19]. This spectrometer is used in the Bell Telephone Laboratories (USA). A TWT with a power up to 1 kW, controlled by a modulator, which is in its turn triggered by the programmable pulse sequence generator, is employed as the source of 20 ns UHF pulses. In the recording circuit there is a coherent receiver of the homodyne type with a videoamplifier, a strobe integrator, and a pen recorder. A novel cavity of the gap type, with a high filling factor and a small size, which is convenient for use at 4.2 K, is incorporated in the spectrometer. In the two-pulse variant, τ is varied over the range 0.14–2.4 μs during the recording of the decay of the ESE signal. A waveguide delay line, which makes it possible to diminish by ~30% the dead time of the spectrometer, has been described[20].

Trifunac et al.[21] described an ESE spectrometer for kinetic studies in pulse radiolysis (Argonne National Laboratory, USA). The source of the UHF pulses is a TWT with a power of 10 W, which amplifies the UHF pulses of the klystron generated with the aid of a fast-response (10 ns) switch. The 90° pulse then has a duration of 30–100 ns, and generates a field $H_1 \cong 1$ G in a cavity of the reflecting type. The circuit employs two further fast-response switches to protect the detecting section of the spectrometer from overload pulses. A low noise TWT or a unipolar amplifier based on field effect transitors can be used in the detector. A characteristic feature of the spectrometer is its employment together with a 3 MeV Van de Graaff accelerator, which makes it possible to irradiate the specimens by intense electron pulses lasting 5–100 ns with a current of ~2 A in the pulse. In a specimen having a volume of 10^{-4} litre, such pulses give rise to a radical concentration of ~10^{-3} M in aqueous media. In kinetic experiments the time interval between the electron pulse and the first 90° UHF pulse was varied. Remote control was used for the part of the apparatus located in the zone unprotected from the radiation, this incorporated the UHF system and control units as well as the permanent H_0 magnetic field unit.

It is known that problems associated with the signals from the bulbs or cuvettes containing the test specimen arise in radiation experiments using, for example, the stationary EPR method. A novel procedure for the reduction or even elimination of this signal has been proposed[21]. If the ESE spectrometer operates under signal detection conditions with inclusion of a radiation pulse (A) and without a pulse (B), then the phase of the B signal before accumulation can be inverted so that $A - B$ difference signals containing only the transient component of the EPR spectrum appear in the accumulator. An example of such an experiment has been presented[21] with the exclusion of the long-lived signal in quartz and the isolation of the spectral lines of the short-lived radical $\dot{C}H_2CO_2$-generated when a solution of potassium acetate is irradiated.

Among other spectrometers described in the literature and used at the present time in vigorous research, we shall mention the second instrument of the Argonne Laboratory[22], the analogous spectrometer at Cornell University (USA)[23], and the spectrometer at the University of Houston (USA)[24]. The ESE spectrometer at the Leyden University in Holland[25] is used to investigate triplet states, while in the University of Delft ESE spectrometers for both the 3 cm [26] and 8 cm [27] ranges are used to study modulation phenomena. The complete list of the spectrometers, some of their technical characteristics, and the main fields of the research carried out on them have been published[28].

III. MAGNETIC DIPOLE–DIPOLE INTERACTIONS IN ESE SPECTROSCOPY

The study of the spatial distribution of paramagnetic centres in solids is based on the theory of magnetic dipole–dipole interactions developed in relation to the ESE method. A review of the present state of the theory can be found in the literature[6,7,29,30]. We shall deal only with the results which are most significant for applications.

The surrounding spins k generate at the site of a given spin p a local field ΔH_p which depends on the relative positions of the spins in the lattice and on the changes in the orientation of the surrounding spins as a function of time. The shift of the resonance frequency of two spins $c/S = 1/2$ corresponding to this field is defined thus:

$$\Delta\omega_{pk}(t) = \gamma^2\hbar r_{pk}^{-3}(1 - 3\cos^2\theta_{pk})\, m_k(t) = A(r_{pk})\cdot m_k(t)\,,$$

where m_k is the projection of the spin k onto the direction of the external field H_0 and $\theta_{pk}$the angle between the vector $\mathbf{r}_{pk}$ and the field $\mathbf{H}_0$. For an assembly of spins k, the shifts are added together:

$$\Delta\omega_p(t) = \sum_k \Delta\omega_{pk}(t)\,.$$

The contribution of this interaction to the time-dependent decrease of the spin echo signal amplitude is defined by the relation

$$V(t) = V_0 \left\langle \exp\left[i \int_0^t S(t)\,\Delta\omega_p(t)\,dt \right] \right\rangle_t \Big\rangle_p\,,$$

where $S(t) = 1$ in the time interval $(0, \tau)$ and $S(t) = -1$ in the time interval $(\tau, 2\tau)$ in the two-pulse ESE variant. Averaging with respect to t is carried out over all the realisations of the time-dependent changes in $m_k(t)$ and the averaging with respect to p takes into account the spatial distribution of the spins k relative to the spins p. If there are only two spins p and k separated by a distance r_{pk}, then the contribution due to the dipole–dipole interaction for the spin k to the decrease of the ESE signal of the spin p must also be averaged with respect to time:

$$V_p(t) = \left\langle \exp\left[iA(r_{pk}) \int_0^t S(t)\, m_k(t)\,dt \right] \right\rangle_t\,.$$

The shift of the resonance frequencies of the spins changes as a function of time as a consequence of random spin flips. Such random changes in the resonance frequencies of the spins are called spectral diffusion. Two mechanisms of random spin flips are usually considered: the spin–lattice relaxation process in which the mutual orientation of the spins is altered (flip-flops). In the latter case the spin excitation migrates in space (there is spin diffusion). If the spin–lattice relaxation makes a definite contribution to the random changes in the resonance frequencies, such spin systems are referred to as type T_1 samples. If the spectral diffusion is induced by random spin flips in the course of spin diffusion, such systems are referred to as type T_2 samples.

Another mechanism of phase relaxation due to the dipole–dipole interaction is associated with a specific pulsed influence on the system of spins in the ESE method: a 180° pulse alters the orientation of the local ΔH_p field generated by the spins k, i.e. executes an "instantaneous" shift of the resonant frequency of the spins. This gives rise to relaxation via the so-called instantaneous diffusion mechanism. Even if the spectral diffusion is fully "frozen", the dipole–dipole interaction between the spins results in a decrease of the ESE signals via the instantaneous diffusion mechanism. If during the time of observation the spins k manage to alter their orientation in a random manner (as a result of spin–lattice relaxation or spin diffusion), they contribute to the decrease of the ESE signal via both instantaneous and spectral diffusion mechanisms. The contribution of the instantaneous diffusion mechanisms depends very greatly on the amplitude H_1 and the duration τ_p of the UHF pulses on the relation between the amplitude of the UHF field H_1 and the overall width and form of the EPR spectral line $[g(\omega)]$.

The random spin flips are described within the framework of various model time distributions. Either an identical average flip rate w is then assumed for all the spins or a distribution of the spins with respect to the flip rate is introduced, for example of the form

$$\varphi(W)\,dW = \left(\frac{3W_{\max}}{2\pi}\right)^{1/2} W^{-3/2} \exp\left(-\frac{3W_{\max}}{2W}\right) dW\,, \qquad (1)$$

where $W_{\max}$ is the most probable flip rate. Using such time distributions, the decrease of the ESE signal has been calculated for the model case of a uniform distribution of spins in space[29].

The paramagnetic centres can be distributed in the lattice of a solid either uniformly or non-uniformly. In the former case they can be stabilised with identical probabilities at any lattice site. For example, a distribution of this type has been observed in frozen vitreous dilute solutions of stable radicals or complexes of paramagnetic ions. The spatial distribution of the paramagnetic centres can be described with the aid of a pair distribution function for the particles $m(r)$, which characterises the probability of finding a paramagnetic centre at a distance r from a specified paramagnetic centre.

If the paramagnetic species are distributed in the specimen in pairs and the distribution with respect to distance within the pairs is specified by the function $n(r)$, then the decrease of the ESE signal is described by the expression

$$V(2\tau) = \int V_p(2\tau, r)\, n(r)\, d^3\mathbf{r}\,.$$

For a uniform distribution of species in the specimens with an average concentration c_{av}, we obtain[29]

$$V(2\tau) = \exp\left\{-c_{cp}\int d^3\mathbf{r}\,[1 - V_p(2\tau, r)]\right\}.$$

The problem of the description of the kinetics of the decay of the ESE signal due to magnetic dipole–dipole interactions of the species is solved in this way in the general case. As a rule, the solution for a wide range of times τ can be obtained only numerically. Hitherto, a wide range of model problems have been analysed in which the spatial distribution of the paramagnetic centres was varied and different types of random processes were employed to describe spectral diffusion[29,31].

The results for systems with a uniform distribution of paramagnetic species are of greatest practical value. For such systems, there is a possibility of a comparison with experiment. They serve as reference standards in the case of a non-uniform distribution of species. Calculation of the rate of decay of the ESE signal owing to the dipole–dipole interactions for a uniform distribution has been carried out for a single spin-flip rate W and for a distribution with respect to rates of type (1). In the latter case, the kinetic expression for example, assumes the form

$$V(2\tau) = \exp\left\{10^{-18}c_{cp}\left[Q_B(\tau, W_{max}) + \left\langle \sin^2\frac{\theta}{2}\right\rangle_{g(\omega)} Q_A(\tau, W_{max})\right]\right\},$$

where $\langle\ldots\rangle_{g(\omega)}$ denotes averaging with respect to the distribution $g(\omega)$ of the frequencies in the EPR spectrum. The exponent, proportional to Q_B, reflects the contribution of spectral diffusion to the decay of the ESE signal and that proportional to Q_A reflects the contribution of the instantaneous diffusion mechanism. The quantities Q_A and Q_B have been calculated numerically as a function of τ and W_{max} and have been published[29,30].

The experimental decay of the ESE signal in the two-pulse method is associated not only with the dipole–dipole interactions between the electron spins but also with the influence of the nuclei of the matrix and of the spin–lattice relaxation on the phase relaxation of the spins. These mechanisms make a signficant contribution to the decay of the ESE signal amplitude and in practice limit the time interval in which the study is carried out from the "ringing" time of the cavity (~0.3 μs) to τ = 2–3 μs. In this interval, the functions Q_A and Q_B can be represented by linear functions in τ for the rates W_{max} in the $0-10^4$ and 10^3-10^5 s^{-1} ranges. This makes it possible to represent the decay of ESE signal in a general form for systems with a uniform distribution[6,7,30]:

$$V(2\tau) = V(0)\exp(-2b\tau),$$
$$b = b_0 + \left[\alpha_C + \alpha_M\left\langle \sin^2\frac{\theta}{2}\right\rangle_{g(\omega)}\right]c_{av}, \qquad (2)$$
$$b_0 = m\tau^n + T_{2l}^{-1},\quad \alpha_M c_{av} = \Delta.$$

where $m\tau^n$ is the term corresponding to the electron–nuclear interaction, n = 1–2 and T_{2l}^{-1} is the rate of phase relaxation due to the spin–lattice interaction. In the limiting case where the coefficient $\alpha_M = 8.2 \times 10^{-13}$ cm^3 s^{-1} the quantity Δ corresponds to the static dipole line width.

Relations of type (2) have been observed in the study of the phase relaxation of a whole series of systems with a uniform distribution of paramagnetic species[6,7]. By studying the dependence of the rate of phase relaxation on the average concentration and θ for a known EPR spectrum, whose form is determine by the type of $g(\omega)$, it is possible to obtain α_C and α_M. As an example, Fig. 3 presents data for the concentration dependence of the rate of phase relaxation for vitreous solutions of VO^{2+} ions in sulphuric acid and for solutions of the stable diphenylpicrylhydrazyl radical in methanol (77 K) and Fig. 4 illustrates the dependence of the rate of phase relaxation on the quantity $\langle\sin^2\theta/2\rangle$ for the $\dot{C}H_2OH$ radicals in methanol γ-irradiated at 77 K. We may note that for absorbed γ-radiation doses in excess of 2000 Gr, these radicals are stabilised uniformly in the matrix[32].

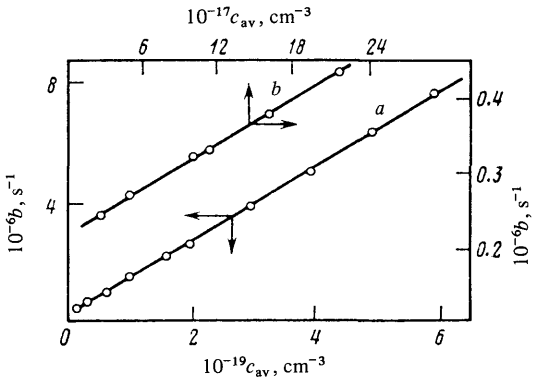


Figure 3. Dependence of the rate of phase relaxation on the concentration of VO^{2+} ions in frozen aqueous sulphuric acid solutions (*a*) and for frozen solutions of diphenylpicrylhydrazyl in methanol (*b*); temperature 77 K.[6,7]

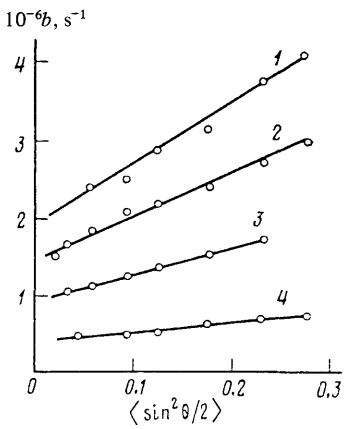


Figure 4. Dependence of the rate of phase relaxation for CH_2OH radicals in methanol (77 K) on the spectrum excitation conditions ($\theta = \gamma H_1 \tau_p$) at different radical concentrations (cm^{-3}): 1) 3×10^{19}; 2) 2.2×10^{19}; 3) 1.3×10^{19}; 4) 0.4×10^{19}. The external magnetic field H_0 is fixed and corresponds to the central line of the triplet in the EPR spectrum of the $\dot{C}H_2OH$ radical[6,7].

Thus, together with the results of the study of the dependence of the ESE signal amplitude on τ, the investigator obtains a fairly complete set of experimental data characterising the physical mechanism of the phase relaxation in the spin system. The factor important for applications is that the study of phase relaxation leads in its turn also to procedures for the investigation of spatial distribution of paramagnetic centres in solids.

In conformity with the foregoing, the spatial distribution of species determines the rate of decay of the ESE signal in the two-pulse method. As for any inversion problem, it is not possible to obtain directly from the rate $V(2\tau)$ information about the relative spatial distribution of species in the test system, which can be characterised, for example, by the pair distribution function $n(r)$ [$n(r)$ is the probability of finding species at a distance r from one another]. There exist two procedures which facilitate this problem. The first involves the calculation of $V(2\tau)$ for different $n(r)$. A series of interesting results have been obtained recently in this way, but these require a direct experimental test[31]. The second procedure involves modelling the function $n(r)$ investigated by a known function for a uniform distribution of species in a limited isolated volume, which corresponds to the introduction of the concept of a local concentration c_{loc}. If it is assumed that the species are for some reason localised uniformly in a volume $v_{loc} < v_0$, where v_0 is the volume of the specimen, then the decay of the ESE signal can be formulated thus:

$$V(2\tau) = \exp\{-c_{loc} \int d^3r[1 - V_p(2\tau, r)]\}$$

and one can assume subsequently that, in terms of this approximation for systems with a non-uniform distribution of species, relations of type (2) hold, where the quantity $c_{loc} = c_{av}v_0/v_{loc}$ is used as the concentration. Such model concepts concerning the spatial inhomogeneity or the presence of c_{loc} are widely used in the study of radical tracks in irradiated solids.

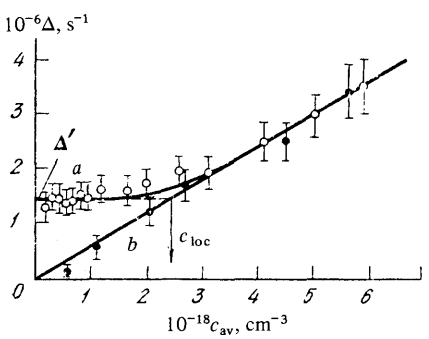


Figure 5. Dependence of the dipole line width Δ on the average concentration of the O^- radical-ions stabilised after the β-irradiation (*a*) and γ-irradiation (*b*) of 9 M aqueous NaOH solutions at 77 K.[33] The local concentration can be obtained from the value of Δ' or from the region of the inflection in the $\Delta(c_{av})$ curve, where $c_{av} = c_{loc}$.

We shall consider briefly only the most significant results obtained recently.

Track effects are manifested most strikingly in the study of the dependence of the relaxation time on the adsorbed dose D or on the average radical concentration in the course of irradiation ($c_{av} = G_R D$, G_R is the radiation yield of the radicals). A typical result for the O^- radical-ions, formed together with the captured electron on β-irradiation of an aqueous 9 M NaOH solution at 77 K, is illustrated by curve *a* in Fig.5.[33] In this system the kinetics of the phase relaxation for the O^- radical-ion are described by Eqns.(2), where $n = 2$, and the main contribution to the rate of phase relaxation comes from the instantaneous diffusion mechanism. The rate of phase relaxation p and the dipole width Δ hardly change at low radical concentrations (before the overlap of the tracks). Subsequently, when the absorbed dose and the overall concentration increase, the dipole interaction between the radicals in different tracks becomes significant. These parameters (*b* and Δ) begin to vary linearly as a function of the average concentration, as for a uniform distribution of radicals or for γ-irradiated specimens (Fig.5, curve *b*), where the track effect can be manifested only for very small absorbed radiation doses.

Track effects had not been observed either in the study (in the course of γ- and β-radiolysis) of the concentration dependence of the rate of relaxation for another particle stabilised in this system, namely the captured electron.

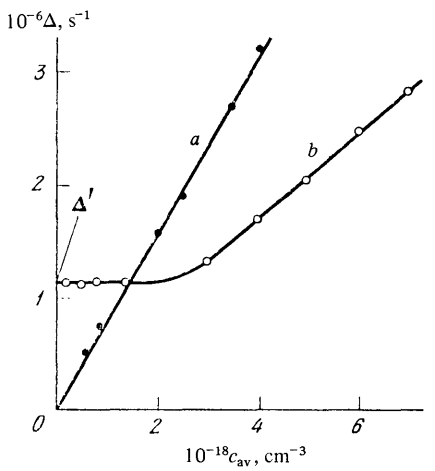


Figure 6. Dependence of the dipole line width on the concentration of paramagnetic species observed on β-irradiation of 1 M solutions of Cd^{2+} ions in methanol at 77 K:[34] *a*) Cd^+ radical-cations; *b*) $\dot{C}H_2OH$ radicals.

IV. RADICAL TRACKS

When the specimen is irradiated, th ionising particle generates positively charged ions and electrons along its path in the solid. As a result of a series of chemical reactions, these primary radiolysis products can be transformed into free radicals or atoms forming a spatially localised track. The appearance of such tracks, particularly for particles with a high ionisation intensity (α- and β-particles, products of nuclear reactions), has been observed and investigated by ESE in studies which have already been reviewed[6,7,12].

Fig.6 presents the results of studies of methanol with added Cd^{2+} ions (0.1–1.0 M), which function as acceptors of the captured electrons. Data for track effects had been obtained earlier for the $\dot{C}H_2OH$ radicals in methanol frozen at 77 K and for its acid solutions[6]. A system with an acceptor proved to be more informative: it was possible to investigate the phase relaxation of both methanol radicals and the Cd^+ radical-cations, because their EPR spectra overlap only partially. A detailed study of the phase relaxation for these species has been carried out[34]. Analysis of the instantaneous diffusion

mechanism yielded the dependence of the dipole line width Δ on the absorbed dose or on the concentration during irradiation (Fig. 6).

The local concentrations of the radicals in the track can be determined from the dipole broadening Δ' in the region of track effects or from the concentration of radicals corresponding to the transition region where $c_{av} = c_{loc}$:

$$c_{loc} = \Delta'/\alpha_p \ .$$

The value of α_p can be determined in experiments for the same systems with a uniform distribution of radicals (γ-irradiation). Assuming further that the radical track is an infinitely long cylinder in which the species are distributed unformly, it is possible to determine the radius of such a track:

$$R_{tr} = \left(\frac{G_R \cdot \overline{LET}}{100\pi c_{loc}}\right)^{1/2}$$

where LET is the average linear energy transfer for the given type of radiation.

For a limited volume of any shape, the contribution of the dipole–dipole interaction to the decay of the ESE signal differs from the contribution for an infinitely large specimen even if the species are distributed uniformly within a limited volume. The corrections R_{tr} due to this effect have been calculated[35]. The quantity G_R is determined independently by the stationary EPR method from the average concentrations of radicals for different irradiation doses (radical accumulation curve). Naturally, when the linear dependence on the rate of relaxation or Δ on the concentration is observed over the entire experimental range of doses, then there is a possibility only of estimates of the upper limit to the values of R_{tr}.

The study of phase relaxation makes it possible to determine the local concentration of paramagnetic species in the solid up to 10^{17}–10^{18} cm^{-3}. In certain cases, for example, for hydrogen atoms[36], it is possible to measure concentrations up to 10^{16} cm^{-3} if the method of consecutive series is used, in which the kinetics of the recovery of the ESE signal are investigated as a function of the repetition frequency of a series of UHF pulses. The kinetics of the restoration of the ESE signal are in this case determined by the spin–lattice relaxation and the spin diffusion; the latter depends also on the intensity of the dipole–dipole interaction between the paramagnetic species, which leads to possibilities for estimating c_{loc}.

The kinetics of the spin–lattice relaxation as a function of the concentration of the paramagnetic species in α- and β-irradiated 8 M solutions of sulphuric acid have been investigated[36] at 77 K. The same local concentrations of hydrogen atoms (10^{18} cm^{-3}) were found for the α-tracks as in the study of the phase relaxation in the given system[37]. In contrast to the earlier investigation[37], for β-irradiation it was possible to obtain a more accurate estimate of the local concentrations: $[\dot{H}]_{loc} = 1^{+1.0}_{0.5} \times 10^{16}$ cm^{-3}.

Thus data have now been obtained about the radical tracks in alkaline, acid, and alcoholic glasses. The mechanism of the radiolysis in these systems has been investigated fairly thoroughly and includes mainly ionic and radical stages leading to the stabilisation of radicals of two types at low temperatures—formed as a result of the reactions of secondary electrons [$\dot{R}(-)$] and those formed by the reactions of positive ions [$\dot{R}(+)$].

In alkaline glasses the precursor of the captured electron e_t is a secondary electron e^- and the precursor of the O^- radical-ion is the H_2O^+ ion[38]:

$$H_2O \rightsquigarrow H_2O^+ + e^- ,$$
$$e^- \rightarrow e_t^- ,$$
$$H_2O^+ + H_2O \rightarrow H_2O + H_2O^+ ,$$
$$H_2O^+ + OH^- \rightarrow H_2O + \dot{O}H ,$$
$$\dot{O}H \rightarrow H^+ + O^- \ .$$

In acid glasses the main radical formation processes can be represented schematically as follows[39]:

$$SO_4^{2-}, (H_2O) \rightsquigarrow SO_4^-, (H_2O^+) + e^- ,$$
$$e^- \rightarrow e_t^- ,$$
$$e_t^- + H^+ \rightarrow \dot{H} ,$$
$$H_2O^+ + SO_4^{2-} \rightarrow H_2O + SO_4^- .$$

In this case the precursor of the $\dot{H}$ atom is a secondary electron and the precursor of the SO_4^- radical-anions is the ionised state of water or SO_4^{2-}. For methanol solutions with Cd^{2+}, the precursors of radical species can also be readily identified, because the main processes are described by the following scheme:

$$CH_3OH \rightsquigarrow CH_3OH^+ + e^- ,$$
$$e^- \rightarrow e_t^- ,$$
$$e_t^- + Cd^{2+} \rightarrow Cd^+ ,$$
$$CH_3OH^+ + CH_3OH \rightarrow CH_3OH_2^+ + \dot{C}H_2OH \ .$$

In the system indicated, it is possible to use the ESE method to investigate the spatial distribution of radicals of two types: $\dot{R}(+)$ and $\dot{R}(-)$. Data for γ-irradiation are compiled in the Table, which reveals the following features: (1) the tracks for the radicals $\dot{R}(+)$, whose precursors are positive ions, have radii of 30–50 Å and are characterised by a local radical concentration of 10^{18}–10^{19} cm^{-3}; (2) if the precursor of the radical is a secondary electron, then the size of the radical track increases to values exceeding 100 Å or more and the local concentration corresponding to doses greater than 5×10^3 Gr is equal to the average concentration; (3) the radiation yields $G_{\dot{R}(+)}$ and $G_{\dot{R}(-)}$ in the systems investigated are almost equal.

The radiation yields of the radicals, their local concentrations, and dimensions of the tracks for certain β-irradiated polar solutions frozen at 77 K.[33–37]

Solution	$\dot{R}(+)$	$\dot{R}(-)$	G_R (for 100 eV)	$10^{-16} c_{loc}$, cm^{-3}	R_{tr}, Å
8 M H_2SO_4	SO_4^-	—	1.5	600	30
8 M H_2SO_4	—	$\dot{H}$	1.5	1	400
9 M NaOH	O^-	—	2.6	400	50
9 M NaOH	—	e_t^-	2.7	20	160
1 M Cd^{2+} in CH_3OH	$\dot{C}H_2OH$	—	2.5	1000	25
1 M Cd^{2+} in CH_3OH	—	Cd^+	2.5	30	130

These data can be accounted for by a detailed analysis of the elementary stages involving the formation, transport, and stabilisation of the radical radiolysis products in the

systems investigated. The radius of the radical track of the $\dot{R}(+)$ species is determined both by the size of the ionisation region and by the positive charge migration reactions. The spatial distribution of the species $\dot{R}(-)$ is determined by the path traversed by secondary electrons before their thermalisation and capture by a trap or an acceptor and by the reverse recombination reaction. A detailed discussion of these problems is outside the scope of this review; it can be found in other publications[34,40-42]. We shall only mention that the results obtained by the ESE method can be regarded as direct confirmation of the model ideas concerning the spatial distribution of radicals in the track of a charged particle, which were put forward as early as the 1950s by Lea[43], Gray[44], and Frolich and Platzman[45].

Studies have also been made on methanol with a Cd^{2+} acceptor on irradiation with species having higher values of LET than for β-particles[40]. Two interesting results were obtained. Firstly, a wide range of absorbed doses was observed in which the rate of phase relaxation is independent of the dose, namely up to concentrations $[\dot{C}H_2OH] \simeq 1.5 \times 10^{19}$ cm^{-3}, which indicates higher values of c_{loc} for these systems. Secondly, it was found that only 10–20% of the $\dot{C}H_2OH$ radicals are involved in the generation of the ESE signal, while the remaining species have phase relaxation times $T_2 < T_{2,min}$ (in the experiments considered $T_{2,min} =$ 400 ns) and do not contribute to the amplitude of the ESE signal. Evidently the local concentration of radicals with short T_2 is greater than 10^{19} cm^{-3}. It has been suggested that they are stabilised in the central part of the track.

An important confirmation that such radical stabilisation is inhomogeneous with respect to the radius of the track has been provided by experiments on photoannealing in such systems. Under the influence of ultraviolet light, the Cd^+ radical-cations interact with methanol, which results in the formation of $\dot{C}H_2OH$ radicals which have a random, uniform spatial distribution in the matrix as a consequence of a series of photochemical reactions and diffusion. Fig. 7 illustrates the variation of the amplitude of the ESE signal for the $\dot{C}H_2OH$ radicals during photoannealing. Partial recombination leads to some decrease of the radical concentration determined by the stationary EPR method. On the other hand, the intensity of the ESE signal increases by a factor of six. The diffusion of radicals from the dense part of the track increases their phase relaxation time, which leads in its turn to an increase of the intensity of the ESE signal.

The experiments described show that the radical track has a complex three-dimensional structure and the hypothesis that they consist of cylinders with a uniform distribution of paramagnetic species can be adopted for the interpretation of experimental data only as a first approximation.

In the general case the local concentration constitutes an average characteristic of the spatial distribution of the species. The interpretation of its changes in the course of chemical reactions has not gone beyond qualitative conclusions, which nevertheless proved extremely useful for the understanding of the mechanisms of reactions in solid matrices. It has been shown recently that more detailed information about the relative spatial distribution of species can be obtained by the relaxation probe method and double electron–electron resonance in ESE spectroscopy.

V. THE RELAXATION PROBE. INVESTIGATION OF THE DISTRIBUTION WITH RESPECT TO DISTANCES IN RADICAL–ION PAIRS

Under the influence of light and radiation, paramagnetic species are frequently formed and stabilised as pairs in solids. Different pairs arise both from decomposition of the excited state M* and from ionisation. For example, if the electron is stabilised in the solid phase, the photoionisation of the Ion M^{n+} can give rise to the pairs $M^{(n+1)+}...e_t^-$. The form of the distribution function for such pairs with respect to distance is determined by the lengths of the paths traversed by the electrons, the rates of the reverse electron–ion recombination reaction and the reactions involving electrons and generating atoms or radicals, the diffusion of the latter to their stabilisation sites, and other experimental conditions, i.e. in the general case by the same factors as the geometry of the radical tracks.

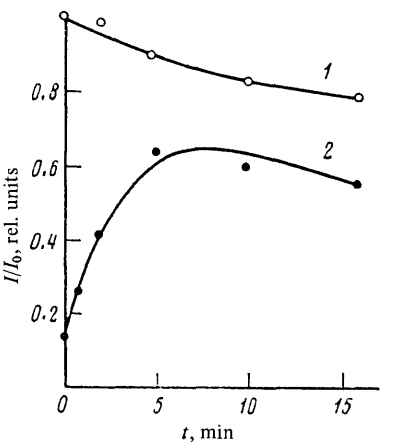


Figure 7. Variation of the relative amplitude I/I_0 of EPR (curve 1) and ESE (curve 2) signals for the $\dot{C}H_2OH$ radicals during photoannealing at 77 K. Specimen—methanol irradiated with α-particles and the ^{7}Li recoil nuclei generated in the reaction $^{10}B(n, \alpha)^7Li$;[40] t = annealing time.

It has been shown in a series of studies[46-51] that the ESE method makes it possible to determine $n(r)$ or to study the properties of this distribution in the case where one of the components of the pair is a species, usually a paramagnetic ion, with a short spin–lattice relaxation time: $T_1 \ll \tau \simeq 10^{-6}$ s.

The main idea of the experiment can be illustrated in the following manner. Radical pairs can be roughly divided into two types. In the pairs of the first type the radicals are close to the ion, within a "black sphere". Owing to the magnetic dipole–dipole interaction with the ion, these radicals have short phase relaxation time T_2^S and make a very small contribution to the intensity of the ESE signal. The main contribution comes from the radicals at large distances from the ion, outside the "black sphere", and having a long relaxation time T_2^l (Fig. 8a). The volume of the "black sphere" is defined by the relation

$$V_B = {}^4/_3\pi R^3 \simeq {}^4/_3\pi \left[\frac{2}{3}\gamma^4\hbar^2 S(S+1)\tau_0 T_1\right]^{1/4} \qquad (3)$$

where τ_0 is the time interval between the first and second pulses, which is fixed and is chosen to be the smallest possible, and S is the spin of the ion. Since the relaxation time of the ion T_1 depends on temperature, the radius of the "black sphere" is also a function of temperature and τ_0. The ESE signal intensity depends on the form of the pair distribution function $n(r)$. This dependence is illustrated in Fig. 8c which shows how the ESE signal intensity varies with

temperature or with the distance from the ion to the radical in two cases—for the uniform $[n^1(r)]$ and non-uniform $[n_2(r)]$ distributions of the pairs with respect to the distances r. In these experiments the paramagnetic ion behaves as the "probe" of the pair distribution: by altering the temperature and following the signal intensity for the known temperature variation of T_1, it is possible to determine $n(r)$.

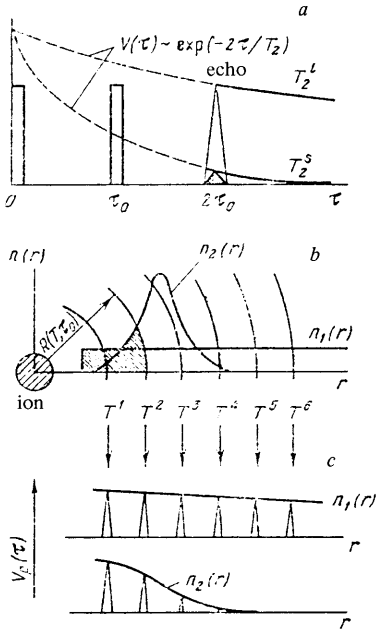


Figure 8. Scheme illustrating the method for the determination of the distribution function with respect to distances in ion–radical pairs from ESE data: *a*) two types of ESE signals arising for a fixed τ from radicals close to the ion (low values of $T_2 = T_2^S$) and remote from the ion (high values of $T_2 = T_2^l$); *b*) schematic representation of the pair distribution function for uniform $[n_1(r)]$ and non-uniform $[n_2(r)]$ distributions; R = radius of the "black sphere" which is different for different temperatures T^i; *c*) dependence of the ESE signal intensity on temperature or distance for two types of $n(r)$.

A theory and methods for the interpretation of the experimental results, which permit the determination of $n(r)$ by the relaxation probe method, have been developed[47,48]. According to the analysis carried out, the function $n(r)$ is given approximately by the relation

$$n(r) = -\frac{d}{dV_B}\left[\frac{V_p(2\tau)}{V_p(0)}\right], \qquad (4)$$

where $V_p(2\tau)$ is the intensity of the ESE signal of the radical in pairs with the ion at a given temperature and for time intervals $\tau = \tau_0$ between the UHF pulses. The quantity V_B, which has the dimensions of volume, is determined experimentally for the same values of the parameters from the relation

$$V_B = -\frac{1}{c_{av}}\ln\left[\frac{V(2\tau)}{V(0)}\right],$$

where $V(2\tau)$ is the spin echo signal intensity for a uniform distribution of the same ions and radicals relative to one another and c_{av} is the average concentration of ions. The distance r is calculated from Eqn.(3).

Thus the experiment reduces to the measurement of the relative intensity of the ESE signal for a fixed τ_0 and different temperatures (1), the measurement of the same quantity for the same system with a uniform distribution of spins (2), and the study of the temperature dependence of T_1 for the ion and V_B(3). The function $n(r)$ is determined by differentiating the experimental curve in accordance with Eqn.(4). The relative accuracy of this method of determination of $n(r)$ is estimated as being to within 30% and the resolving power with respect to r is ~1 Å.[46–48] The relaxation probe method has found applications in studies of the steric characteristics of the formation, diffusion, and reactions of the radicals formed on photolysis and radiolysis of matrices.

1. Distribution of Radicals in Photolysis and Radiolysis

The most detailed information about the function $n(r)$ can be obtained for ions with a fairly short relaxation time $T_1 \ll 10^6$ s. Such ions include Fe^{2+}. A detailed study has therefore been made[47,48] of the pair distribution of the species arising on photolysis of the Fe^{3+} ion in vitreous alcohol matrices via the overall reaction

$$Fe^{3+} + R_2CH(OH) \xrightarrow{h\nu} Fe^{2+} + R_2\dot{C}OH + H^+,$$

where R = H for methanol and R = CH_3 for isopropyl alcohol.

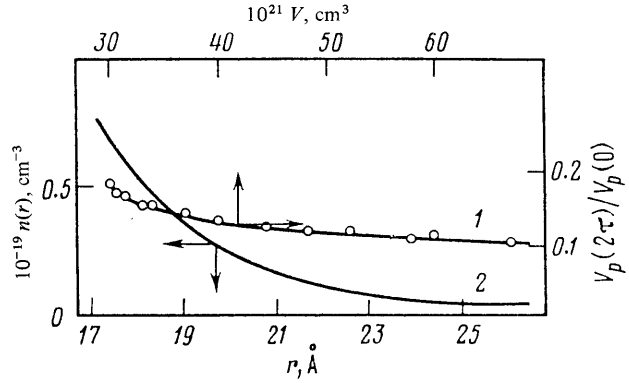


Figure 9. Dependence of the relative ESE signal amplitude $V_p(2\tau)/V_p(0)$ on the volume V_B (curve *1*) and the corresponding pair distribution function (curve *2*) for the Fe^{2+}... $\dot{C}H_2OH$ pairs in methanol irradiated with ultraviolet light[47].

Specimens of two types were investigated—with a spatial distribution of species in pairs (photolysis on irradiation with light at $\lambda > 330$ nm) and with a uniform distribution of radicals. The latter were obtained by photolysis with the unfiltered light of a DRSh-500 lamp, which led to the decomposition of the alcohol radicals into lighter species (for example, CH_3 and HCO in the case of methanol), their diffusion, and their secondary reactions with the matrix. Data were obtained for the dependence of the relative ESE signal amplitude $V_p(2\tau)/V_p(0)$ on temperature and the volume V_B of the "black sphere" (Fig.9, curve *1*). Eqn.(4) makes it

possible to determine the distribution function with respect to radical–ion distances in these experiments (Fig. 9, curve 2). For methanol, the function $n(r)$ was found in the range of values of r from 17 to 26 Å; in this range it decreases exponentially with a characteristic descent parameter of 3 Å. Analogous results were obtained also for solutions of Fe^{3+} in isopropyl alcohol.

The analytical form of the functions $n(r)$ in the experiments described cannot be determined for Fe^{2+} ions in the range $r < 17$ Å. The resolving power of the method in the region of short distances (r_{min}) is determined by the possible experimental values of τ_0 and T_1. For $\tau_0 = 0.3 \times 10^{-6}$ s and $T_1 = 10^{-11}$–10^{-10} s, Eqn. (3) yields r_{min} 10–15 Å for ferrous ions. The upper limit, corresponding to $T_1 \cong \tau_0$, is then $r_{max} \cong 70$–100 Å. For the most interesting range $r < 17$ Å, there is, however, a possibility of another approach to the experimental estimation of the form of the function $n(r)$.

If the spin–lattice relaxation time of the ion T_1 is known, it is possible to estimate the relative number of radicals in the region of rapid relaxation (for $r < r_{min}$) by studying the changes in the ESE signal intensity on transition from a non-uniform spatial situation involving pairs to a uniform situation. This can be readily achieved by annealing the specimen at temperatures such that the radical–ion pairs begin to move apart without a significant contribution of recombination. Only an increase of the ESE signal intensity with increase of temperature is observed in such experiments. The constancy of the overall concentration of radicals N_0 is monitored simultaneously by the stationary EPR method. By varying T_1 or τ_0, i.e. the radius of the "black sphere", one obtains a histogram of the spatial distribution—the quantity $\Delta N(r)/N_0$. According to these experiments[47,48], 80% of the total number of Fe^{2+}... $R_2C(OH)$ pairs are located in the range $r < 17$ Å in methanol and isopropyl alcohol (Fig. 10*a*).

Analysis of the mechanism of the formation of radicals in frozen solutions in alcohols containing Fe^{3+} ions[52,53] showed that, when light is absorbed by the ion introduced into the alcohol in the form of a halogen complex, phototransfer of an electron from a matrix molecule to the complex takes place. Such phototransfer is apparently most likely for the alcohol molecules closest to the complex. The data obtained by the ESE method (Fog. 10*a*) concerning the mutual spatial distribution of ions and radicals are therefore consistent with the hypothesis of the phototransfer of an electron from the matrix. However, since the characteristic average distance in the ion–radical pairs is ~12 Å, one must assume that the radicals are not stabilised at the site of their formation in the first coordination sphere of the complex but execute several jumps up to the stabilisation site. This also gives rise to a set of distances characterising the function $n(r)$, which describes the "tail" of the distribution (Fig. 9).

The pair distribution of the species formed on photolysis of M^{n+} ions (where $M^{n+} = Fe^{2+}$ or Cr^{2+}) in glasses of an aqueous solution of sulphuric acid has been investigated by the ESE method[46,49]:

$$M^{n+}(H_2O) \xrightarrow{h\nu} M^{(n+1)+} + \dot{H} .$$

The relaxation time T_1 for these ions is ~10^{-7} s and does not differ significantly from the limiting value $\tau_0 \cong 10^{-6}$ s. It is therefore not possible to determine the detailed form of the function $n(r)$. It has been found by the method involving the isothermal annealing of the specimen that ~80% of the atoms are located at distances from the ion up to 50 Å.

A change in the line shape of the H and D atoms has been observed[49] in the stationary EPR spectrum during annealing. This effect has also been attributed to the characteristic pair distribution of species in the system investigated. Its analysis makes it possible to refine significantly the distribution of the pairs: approximately 30% of the total number of pairs should have distances from 0 to 17 Å. The histogram which follows from the ESE and EPR data on the system indicated is illustrated in Fig. 10*b*.

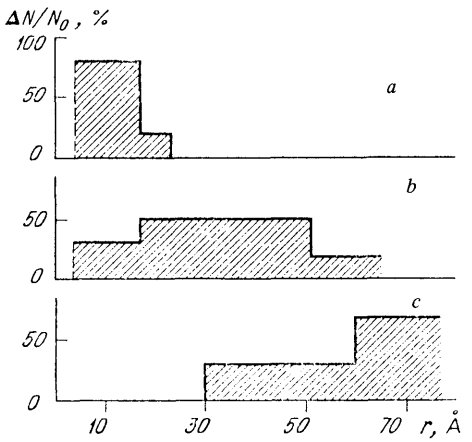


Figure 10. Histograms of the distribution with respect to the distances r in the radical–ion pairs formed on photolysis (*a* and *b*) and radiolysis (*c*) of polar frozen solutions (according to the data in Refs. 46–49): *a*) $Fe^{3+} + RHOH \xrightarrow{h\nu} Fe^{2+}$... ROH (R = CH_2, $(CH_3)_2C$); *b*) $M^{2+} + H_2SO_4 \xrightarrow{h\nu} M^{3+}$...H (M = Fe, Cr); *c*) $D_2SO_4 \xrightarrow{\gamma} \dot{D}$... SO_4^-.

Two alternative mechanisms for this photochemical reaction have been discussed[54]. According to one of them, the primary reaction step is electron transfer to the water molecule closest to the ion. After this, the H_2O^- species either decomposes into H and OH^- or reacts with H_3O^+ to form H. In the second mechanism, a mobile electron is formed under the influence of light, diffuses through the matrix, and reacts with the acceptor. Recently published experimental data[54,55] support the first mechanism.

If the mobile electron is not formed in the primary step (i.e. the first mechanism is valid), the experimental spatial distribution of H atoms relative to the Fe^{2+} and Cr^{2+} ions implies that the atoms are not stabilised at the site of their formation and diffuse until they are captured by a trap. The distribution function for the pairs with respect to distances has the following form for a model of this kind[56]:

$$n(r) = [4\pi r_0^3 r]^{-1} \cdot \exp[-r/r_0] .$$

It was found that the function describes equally well data obtained by the ESE method and EPR with $r_0 = 15$ Å.

The distribution $n(r)$ for the pairs SO_4^-... H(D), formed on γ-radiolysis of an aqueous solution of sulphuric acid, has been investigated[50]. In this case the mechanism of the formation of the pairs is associated with the ionisation of SO_4^{2-} and H_2O (D_2O) and the capture of a secondary electron by the $H^+(D^+)$ ion. In the determination of $n(r)$ in an analytical form, the same difficulties arise as for the ions Fe^{3+} and Cr^{3+}, since $T_1 = 10^{-6}$ s for SO_4^-. Analysis of the kinetics of the decrease of the ESE signal for the $\dot{D}$... SO_4^- pairs showed that the fraction of pairs with distances from 0 to 60 Å is ~30%. On the basis of considerations concerning the

possible lengths of the paths traversed by a secondary electron, the function describing the distribution of secondary electrons with respect to distances[41], as well as data for the experimental yield of pairs, it has been concluded[50] that a region $0 < r < 30$ Å with zero values of $n(r)$ exists as a result of primary recombination in the spatial distribution of pairs. The histogram for this case is illustrated in Fig.10c.

Thus the series of experiments carried out by the ESE method made it possible to obtain for the first time direct information about the spatial pair distribution of the paramagnetic species formed on ultraviolet and γ-irradiation of a series of polar substances.

2. Diffusion of Radicals

As a result of diffusion, the paramagnetic centres gradually emerge from the "black sphere" near the ion and their phase relaxation times increase, which leads to an increase of the ESE signal intensity for a fixed τ_0. Ultimately, the ESE signal intensity reaches a constant value at long times which corresponds to a uniform distribution of radicals in the system.

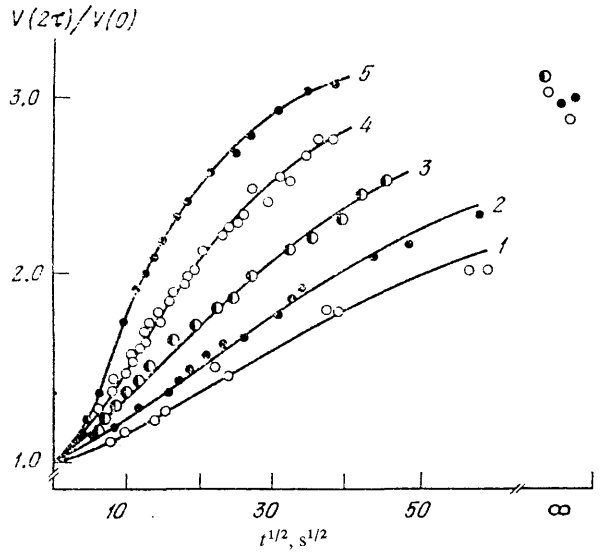


Figure 11. Increase of the ESE signal intensity during the annealing at different temperatures of specimens with $Fe^{3+}...H$ pairs arising on photolysis of Fe^{2+} solutions in 7 M H_2SO_4;[46] temperature (K): 1) 90.1; 2) 91.3; 3) 93; 4) 95; 5) 97.

The dependence of the ESE signal intensity on the annealing time at different temperatures has been investigated[46] for the $Fe^{3+}...\dot{H}$ pairs formed on photolysis of Fe^{2+} ions in frozen solutions of sulphuric acid (Fig.11). The degree of enhancement of the echo signal amplitude on diffusion is determined by the product of the diffusion coefficient of hydrogen atoms and the characteristic annealing time, for example the time of attainment of half the limiting intensity of the ESE signal ($t_{1/2}$) at a given temperature. When the Arrhenius temperature dependence obtains, we have

$$t_{1/2} = D_0^{-1} \exp(E/RT) .$$

$E = 5.5 \pm 0.5$ kcal mol^{-1} and $D_0 = 7 \times 10^{-4}$ cm^2 s^{-1} were found for H atoms from measurements of $t_{1/2}$ at different temperatures in the range 90–100 K.

More detailed information about the mechanism of diffusion in a solid can be obtained by studying the changes in the pair distribution function at different times during diffusion. Such studies have been carried out for radicals in alcohol glasses containing the $Fe^{2+}...R_2\dot{C}OH$ pairs for methanol and isopropyl alcohol[47]. With increased annealing time, the $n(r)$ distribution density tends to zero, as is to be expected from the diffusion equation. This has in fact been observed, for the $Fe^{2+}...\dot{H}$ pairs[46]. In studies of the diffusion of radical–ion pairs in alcohols, it was, however, found that the spatial scale of the diffusion is limited. Starting from a certain instant at a constant annealing temperature, the form of the pair distribution function virtually ceases to depend on the annealing time. This is illustrated by the results of the experimental determination of the pair distribution function with respect to distances at different times, presented in Fig.12*a* for radicals in methanol. For example, at an annealing temperature of 96.5 K, the principal changes in the function $n(r)$ take place during the first two minutes of annealing, which follows from a comparison of curves *0* and *1*. A further increase of annealing time at 96.5 K by an order of magnitude does not entail significant changes in $n(r)$ (curve *2*). An analogous pattern can be observed also in the group of curves characterising the variation of $n(r)$ during annealing at 100 K (curves *3*–*5*). Only an increase of temperature to 112 K results in $n(r)$ close to zero.

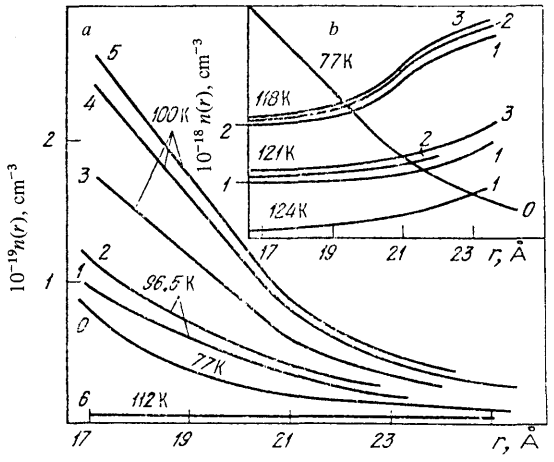


Figure 12. Variation in the course of thermal annealing of the pair distribution function for radical–ion pairs: *a*) $Fe^{2+}...\dot{C}H_2OH$ pairs in methanol; 0) initial $n(r)$ at 77 K; 1) and 2) annealing at 96.5 K for 2 and 20 min respectively; 3)–5) annealing at 100 K for 4, 9, and 19 min respectively; annealing at 112 K for 1 min; *b*) $Fe^{2+}...(CH_3)_2\dot{C}OH$ pairs in isopropyl alcohol; 0) initial $n(r)$. In each group of annealing curves at 118, 121, and 124 K the annealing times are 1, 2, and 6 min for curves *1*, *2*, and *3* respectively.

An analogous picture has been observed for radicals in isopropyl alcohol (Fig.12*b*). The difference from methanol consists only in the fact that, in addition to diffusion, raising the temperature results in a reaction between the radicals

and the ion in which a radical-ion complex is formed. Ultimately the distribution function $n(r)$, established as a result of diffusion and the reaction, does not have a descending form as in the case of methanol but actually increases with increase of r. In the vicinity of the ion a minimum in the distribution density is observed. We may note that the formation of a hydrogen atom–ion complex had been observed earlier for other systems—for iron[57] and copper[58] ions.

The observed characteristics of the diffusion of radicals have been interpreted[47] taking into account the fact that in glasses there are distributions with respect to intermolecular distances, mobilities, and other parameters between different sites. As a consequence of the distribution with respect to diffusion parameters, the radical probably diffuses only as far as the cell which it finds difficult to leave at the given temperature and is trapped there. The higher the temperature the longer the path which it traverses in the search for a suitable trap and the initial pair distribution becomes more diffuse. We may note that analogous characteristics are known for the kinetics of the recombination of radicals in solids: the kinetic curves frequently tend to a limit or have a "stepped" form with a rapid variation of the concentration in the region of short chemical reaction times and a slow change in the region of long chemical reaction times (see, for example, Blyumenfel'd et al.[59]).

3. Changes in the Pair Distribution During Chemical Reactions of Radicals

By studying the pair distribution function in the course of chemical reactions in the matrix by the relaxation probe method, it is possible to infer the scale of the migration of the valence in various elementary steps. Such studies have been carried out for radicals formed on photolysis of Fe^{3+} solutions in isopropyl alcohol[51]. In this system, there is a possibility of various chemical reactions induced by light or by heating the specimen.

Irradiation with light at $\lambda > 330$ nm leads to the formation of pairs consisting of the alcohol radicals $(CH_3)_2\dot{C}OH$ and Fe^{2+} ions. The pair distribution function $n(r)$ in the above reaction has been studied in detail for the range of distances 17–23 Å (as for methanol); the results are presented in Fig.13 (curves *a*). On illumination with light at $\lambda > 300$ nm, the radicals $(CH_3)_2\dot{C}OH$ are transformed into isopropyl radicals $(CH_3)_2\dot{C}H$ by the reaction

$$(CH_3)_2\dot{C}OH + (CH_3)_2CH(OH) \xrightarrow{h\nu} (CH_3)_2\dot{C}H + H_2O + (CH_3)_2CO \ . \quad (5)$$

The concentration of the radicals and the changes in their structure are monitored simultaneously using stationary EPR spectra. After the complete conversion of the alcohol radicals into alkyl radicals, a study was made of the function $n(r)$ for these radicals (Fig.13*b*).

A further three types of reaction can be carried out for the same system on heating or illumination of the specimen and the pair distribution function can be investigated after these transformations. When a specimen containing propyl radicals is heated at 106 K, the substitution reaction

$$(CH_3)_2\dot{C}H + (CH_3)_2CH(OH) \xrightarrow{106\,K} (CH_3)_2\dot{C}OH + (CH_3)_2CH_2 \quad (6)$$

regenerates the alcohol radicals whose pair distribution function is illustrated in Fig.13 (curves *c*). The isopropyl radicals obtained via reaction (5) isomerise under the influence of light at $\lambda > 250$ nm:

$$(CH_3)_2\dot{C}H \xrightarrow{h\nu} CH_3CH_2\dot{C}H_2 \ . \quad (7)$$

In reaction (7) the function $n(r)$ hardly changes and remains close to curve *b* in Fig.13. On the other hand, the propyl alcohol generated by reaction (7) interacts with the matrix at 106 K, regenerating the alcohol radicals:

$$CH_3CH_2\dot{C}H_2 + (CH_3)_2CH(OH) \xrightarrow{106\,K} CH_3CH_2CH_3 + (CH_3)_2\dot{C}OH \ . \quad (8)$$

For the latter, the distribution function proved to be constant and corresponds to a uniform distribution of species.

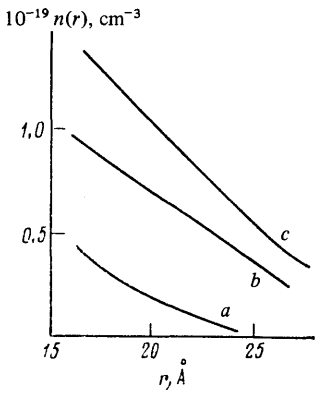


Figure 13. Variation of the form of the pair distribution function $n(r)$ due to chemical reactions in frozen Fe^{3+} solutions in isopropyl alcohol[51]: *a*) initial function $n(r)$ for the $Fe^{2+}...(CH_3)_2\dot{C}OH$ pairs; *b*) the $n(r)$ distribution function for the $Fe^{2+}...(CH_3)_2\dot{C}H$ pairs formed via reaction (5) (see text); this function does not change in reaction (7); *c*) the $n(r)$ function for the $Fe^{2+}...(CH_3)_2\dot{C}OH$ pairs formed in reaction (6).

The spatial migration of the valence for the corresponding reaction can be inferred from the distances between points with identical values of $n(r)$ on the curves in Fig.13. The lattice parameter of isopropyl alcohol is ~4.6 Å. The results presented show that reaction (6) takes place within a "cage" (the valence migrates over a distance of 3–4 Å); in reaction (5) the isopropyl radical is not stabilised at the site of its formation but executes 1–2 jumps before it is captured by a suitable trap (the displacement is by ~8 Å). The propyl radical diffuses over appreciably longer distances (≳20–30 Å) in the course of reaction (8) in the matrix. Within the limits of the accuracy of the measurements, the isomerisation reaction (7) leads to the migration of the valence over distances ≲1 Å.

VI. THE DOUBLE ELECTRON–ELECTRON RESONANCE METHOD IN ESE SPECTROSCOPY AND ITS APPLICATIONS

The spin probe method is applicable for fairly short T_1 of one member of the pair of spins. If the spins *A* and *B* in the pair have similar and fairly long relaxation times T_1, then phase relaxation can be used in the analysis of their spatial distribution, as in the study of radical tracks. However, this is possible only when the difference between the Zeeman frequencies $\omega_A - \omega_B < \gamma H_1$, i.e. under the conditions of the excitation of the complete EPR spectrum.

A method has been proposed[60] for the investigation of the pair distribution of species with similar or even equal T_1 and different ω_A and ω_B. The method is based on the observation of the variation of the ESE signal amplitude for the spins A when the UHF pumping pulse is switched on at a frequency ω_B (Fig.14). Such an influence on the spins B alters the local field at the site of the location of the spin A, by an amount whose magnitude is determined by the dipole–dipole interaction between A and B. Additional dephasing of the precession of the spins A arises, which reduces in its turn the echo signal amplitude A_A due to A compared with its value V_A^0 in the absence of the pulsed pumping of the spins B; thus the UHF pulse at a frequency ω_B stimulates the instantaneous diffusion process. An analogous formulation of the experiment can be found also in NMR spectroscopy[61].

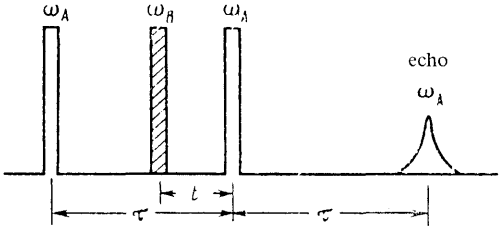


Figure 14. The sequence of the effects of the UHF pulses and the pumping pulse generating the ESE signal in the pulsed double electron–electron resonance method.

A theory of the method has been developed[60] and it has been shown that the experimental ratio V_A/V_A^0, measured for different concentrations of the pairs and extrapolated to zero concentrations of spins (in order to eliminate the decay of the signal owing to the dipole interaction between the pairs), is related to the pair distribution function $n(r)$ by the integral equation

$$[V_A/V_A^0]_{c\to 0} = 1 - p\left[1 - \int_0^\infty 2\pi r^2 n(r) K(u)\, dr\right] \qquad (9)$$

where $p = \langle \sin^2 \theta_B/2 \rangle_{g(\omega B)}$ is the fraction of the spins B excited by a pulse at a frequency ω_B and the averaging is carried out with respect to the EPR spectrum of the species B; $K(u)$ is a function determined by the dipole interactions of the spins of A and B:

$$K(u) = \frac{1}{2}\int_0^\pi \cos[u(1 - 3\cos^2\theta)] \sin\theta d\theta ,$$

where $u = \gamma^2 h r^{-3} t$, θ is the angle between $\mathbf{H}_0$ and the vector $\mathbf{r}$ connecting A and B and t is the time interval between the pulse at a frequency ω_B and a second pulse at a frequency ω_A.

As an example, a study has been made[60] of pairs consisting of hydrogen atoms and the parent hydroquinone radicals formed on photolysis at 77 K of vitreous solutions of hydroquinone in 8 M sulphuric acid solutions. A bimodal cavity of the type already described[62], was used in the ESE spectrometer for such experiments. The specimen was placed at the antinode of the magnetic field for both modes, one of which tuned to the frequency ω_A (hydrogen atoms) and the other to ω_B (hydroquinone radicals). The variation of V_A/V_A^0 was investigated for different times t and radical concentrations c_B. Identical results were obtained for the $\dot{H}$ and $\dot{D}$ atoms.

In the analysis of the experimental data, an approximate calculation of the values of $n(r)$ by Eqn.(9), in which the core $K(u)$ was replaced by a stepped function, was carried out. In this case, graphical differentiation of the experimental curve represented by the expression

$$V(t) = 1 - [1 - (V_A/V_A^0)_{c_B\to 0}]\frac{1}{p}$$

with respect to the parameter $r = (0.83\gamma^2 ht)^{1/3}$ yields the required distribution function in the form $2\pi r^2 n(r)$. The graph of this function, having a maximum at $r \cong 45$ Å, is presented in Fig.15. Its integration shows that 63% of the pairs are contained in the range 0–85 Å. The remaining pairs have $r > 85$–100 Å and the character of their distribution cannot be determined, since they make a small contribution to the $V(t)$ relation.

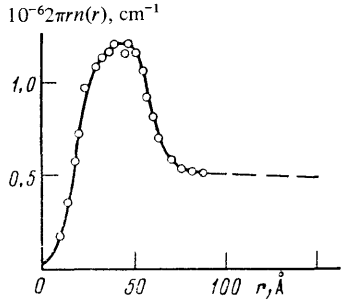


Figure 15. The distribution function with respect to distances for the $\dot{H}$ atom–hydroquinone radical pairs formed on photolysis of hydroquinone solutions in 8 M sulphuric acid frozen at 77 K.[60]

According to Shelimov et al.[63] and Bazhin[64], the paramagnetic species in the above system are formed as a result of the photoionisation of hydroquinone (ArH):

$$ArH + H_2O(H_3O^+) \xrightarrow{h\nu} (ArH^+) + \dot{H} + OH^-(H_2O) .$$

The observed distribution of pairs with respect to distances can therefore be due to two processes: the migration of electrons until their capture by a hydronium ion and the diffusion of hydrogen atoms until their stabilisation in traps. Estimates have shown that the energy of the secondary electron arising on photoionisation of hydroquinone in this system does not exceed 1 eV. For electron energies in the range 1–2 eV, the distances traversed in water are 25 Å.[41] On the other hand, according to the results described above[49], the average diffusion distance to the trap is 30 Å. The maximum of the distribution function for the pairs $(ArH^+)...H$ at $r \cong 45$ Å corresponds to the overall contribution of both processes. Further studies are necessary to elucidate the role of different transport processes in the establishment of an inhomogeneous pair distribution in reactions whose primary stage is photoionisation.

By virtue of its greater universality compared with the relaxation probe method, it is to be expected that the double electron–electron resonance pulse method will find extensive application in the future in studies of the spatial distribution of species.

The results discussed above show that ESE constitutes a direct and informative method for the investigation of the spatial distribution of paramagnetic species in the solid

phase. With the aid of ESE, there is a possibility of both a qualitative approach, yielding information about the possible local radical concentrations, and of studies of characteristics such as the pair distribution function of paramagnetic species and the changes in the latter during diffusion and chemical reactions in a solid.

The physicochemical applications of the ESE method, one of which was examined in the present review, are based on the physical theory of the method, which has been fairly adequately developed at the present time, and a continually improving experimental base. It is to be expected that in the future ESE will occupy among the applications of microwave spectroscopic methods in chemistry a place no less important than that of the stationary EPR spectroscopy.

REFERENCES

1. E.L.Hahn, Phys.Rev., 1950, **77**, 297.
2. E.L.Hahn, Phys.Rev., 1950, **80**, 580.
3. R.J.Blume, Bull.Amer.Phys.Soc.II, 1956, **1**, 397.
4. R.J.Blume, Phys.Rev., 1958, **109**, 1967.
5. W.B.Mims, in "Electron Paramagnetic Resonance" (Edited by S.Geschwind), Plenum Press, New York, 1972, p.263.
6. K.M.Salikhov, A.G.Semenov, and Yu.D.Tsvetkov, "Elektronnoe Spinovoe Ekho i Ego Primenenie" (The Electron Spin Echo and Its Applications), Izd.Nauka, Novosibirsk, 1976.
7. K.N.Salikhov and Yu.D.Tsvetkov, in "Time Domain Electron Spin Resonance" (Edited by L.Kevan and R.Schwartz), Wiley Intersci., New York, 1979, p.231.
8. A.D.Milov, M.D.Shchirov, and V.E.Khmelinskii, Dokl.Akad.Nauk SSSR, 1974, **218**, 878.
9. A.D.Trifunac and J.R.Norris, Chem.Phys.Letters, 1978, **59**, 140.
10. A.D.Trifunac, J.R.Norris, and R.G.Lowler, J.Chem.Phys., 1979, **71**, 4380.
11. W.B.Mims, Rev.Sci., 1974, **45**, 1583.
12. Yu.D.Tsvetkov, Izv.Sibir.Otd.Akad.Nauk SSSR, Ser.Khim., 1976, **4**, 90.
13. A.G.Semenov and V.E.Khmelinskii, Pribory i Tekh. Eksper., 1967, **5**, 197.
14. V.E.Khmelinskii and A.G.Semenov, in "Svobodnoradikal'nye Sostoyaniya v Khimii" (Free-Radical States in Chemistry), Izd.Nauka, Novosibirsk, 1972, p.241.
15. A.L.Buchachenko, "Khimicheskaya Polyarizatsiya Elektronov i Yader" (Chemically Induced Polarisation of Electrons and Nuclei), Izd.Nauka, Moscow, 1974.
16. A.G.Semenov, M.D.Shchirov, V.D.Zhidkov, V.E.Khmelinskii, and E.V.Dvornikov, "Kogerentnyi Spektrometr ESE, Preprint 3" (A Coherent ESE Spectrometer. Preprint 3), IKhKiG Sibir.Otd.Akad. Nauk SSSR, Novosibirsk, 1980, pp.1–25.
17. A.G.Semenov and Yu.D.Tsvetkov, in "Schultegung Modern Methoden der Hochfrequenzspektroskopie, Berlin (DDR), Physikalishe Gesellschaft Der DDR", 1981, p.107.
18. W.E.Blumberg, W.B.Mims, and D.Zuckerman, Pribory dlya Nauch.Issledovanii, 1973, **5**, 10.
19. W.B.Mims and J.Peisach, Biochemistry, 1976, **15**, 3863.
20. J.L.Davis and W.B.Mims, Rev.Sci.Instr., 1981, **52**, 131.
21. A.D.Trifunac, J.R.Norris, and R.G.Lowler, J.Chem. Phys., 1979, **71**, 4380.
22. J.F.Norris, M.D.Thurnauer, and M.K.Bowman, Adv. Biol.Med.Phys., 1980, **17**, 365.
23. A.E.Stilman and R.N.Schwartz, J.Phys.Chem., 1981, **85**, 3031.
24. T.Ichikawa, L.Kevan, and P.A.Narayana, J.Phys. Chem., 1979, **83**, 3378.
25. B.J.Botter, D.C.Doetschman, J.Schmidt, and J.H.van der Waals, Molecular Phys., 1975, **30**, 609.
26. R.de Beer, R.Chatterjee, and R.P.Merks, J.Phys. Chem., 1976, **9**, 1539.
27. R.de Beer and R.P.Merks, Delft Progress Report (Delft), 1979, **4**, 63.
28. W.B.Mims and Yu.D.Tsvetkov, International List of ESE Spectrometers. Preprint of Bell Laboratories, New Jersey (USA), Murray Hill, 1982, pp.1–34.
29. S.A.Dzyuba, K.M.Salikhov, A.M.Raitsimring, and Yu.D.Tsvetkov, "Chislennye Raschety Kinetiki Spada Signala Elektronnogo Spinovogo Ekha za Schet Dipol'–Dipol'nykh Vzaimodeistvii, Preprint 6" (Numerical Calculations of the Rate of Decay of the Electron Spin Echo Signal due to Dipole–Dipole Interactions. Preprint 6), IKhKiG Sibir.Otd.Akad. Nauk SSSR, Novosibirsk, 1980, pp.1–29.
30. K.M.Salikhov, S.A.Druba, and A.M.Raitsimring, J.Magn.Reson., 1981, **42**, 255.
31. V.V.Tregub, A.M.Raitsimring, and V.M.Moralev, "Chislennoe Modelirovanie Prekov Ioniziruyushchikh Elektronov v Vode, Preprint 8" (Numerical Modelling of the Tracks of Ionising Electrons in Water, Preprint 8), IKhKiG Sibir.Otd.Akad.Nauk SSSR, Novosibirsk, 1981, pp.1–35.
32. A.M.Raitsimring et al., Khim.Vys.Energii, 1970, **4**, 369.
33. A.M.Raitsimring, R.I.Samoilova, V.M.Moralev, and Yu.D.Tsvetkov, in "Proceedings of the IVth International Symposium on Radiation Chemistry", Publish.House of Hungarian Acad.of Sci., Budapest, 1976, Vol.691.
34. R.I.Samoilova, A.M.Raitsimring, and Yu.D.Tsvetkov, Int.J.Radiat.Phys.Chem., 1980, **15**, 553.
35. S.A.Dzyuba, A.M.Raitsimring, and Yu.D.Tsvetkov, Zhur.Fiz.Khim., 1979, **53**, 2842 [Russ.J.Phys.Chem., 1979(11)].
36. A.M.Raitsimring and Yu.D.Tsvetkov, Khim.Vys. Energii, 1978, **12**, 122.
37. A.M.Raitsimring, V.M.Moralev, and Yu.D.Tsvetkov, Khim.Vys.Energii, 1975, **9**, 517.
38. A.K.Pikaev, "Sol'vatirovannyi Elektron v Radiatsionnoi Khimii" (The Solvated Electron in Radiation Chemistry), Izd.Nauka, Moscow, 1969, p.289.
39. B.G.Ershov, A.I.Mustafaev, and A.K.Pikaev, Int.J.Radiat.Phys.Chem., 1971, **3**, 71.
40. R.I.Samoilova, A.M.Raitsimring, and Yu.D.Tsvetkov, Khim.Vys.Energii, 1978, **13**, 301.
41. A.M.Raitsimring and Yu.D.Tsvetkov, Khim.Vys. Energii, 1980, **14**, 228.
42. R.I.Samoilova, Candidate's Thesis in Chemical Sciences, Institute of Chemical Kinetics and Combustion, Siberian Division of the USSR Academy of Sciences, Novosibirsk, 1981.
43. D.E.Lea, "Action of Radiation on Living Cells", Cambridge University Press, Cambridge, 1955.
44. L.H.Gray, J.Chem.Phys., 1951, **48**, 172.
45. H.Frölich and L.Platzman, Phys.Rev., 1953, **92**, 1152.
46. P.P.Borbat et al., Fiz.Tverd.Tela, 1977, **19**, 1080.
47. S.A.Dzuba, A.M.Taitsimring, and Yu.D.Tsvetkov, Chem.Phys., 1979, **44**, 357.
48. S.A.Dzyuba et al., Teor.Eksper.Khim., 1978, **14**, 193.
49. V.V.Konovalov, S.A.Dzyuba, A.M.Raitsimring, K.M.Salikhov, and Yu.D.Tsvetkov, Khim.Vys. Energii, 1980, **14**, 525.

50. S.A.Dzyuba, A.M.Raitsimring, and Yu.D.Tsvetkov, Khim.Vys.Energii, 1981, **15**, 37.
51. S.A.Dzyuba et al., Teor.Eksper.Khim., 1979, **15**, 541.
52. V.F.Plyusnin and N.M.Bazhin, Khim.Vys.Energii, 1974, **8**, 316.
53. V.F.Plyusnin, Candidate's Thesis in Chemical Sciences, Institute of Chemical Kinetics and Combustion, Siberian Division of the USSR Academy of Sciences, Novosibirsk, 1974.
54. J.Moan, O.Kaalhus, and B.Hevic, Chem.Phys. Letters, 1979, **61**, 481.
55. V.V.Korolev and N.M.Bazhin, Khim.Vys.Energii, 1978, **12**, 421.
56. A.Mozumder and M.Tachija, J.Chem.Phys., 1975, **62**, 979.
57. N.M.Bazhin and V.M.Berdnikov, in "Svobodnoradikal'nye Sostoyaniya v Khimii" (Free Radical States in Chemistry), Izd.Nauka, Novosibirsk, 1971, p.129.
58. O.B.Kiseleva, V.F.Plyusnin, and N.M.Bazhin, Khim. Vys.Energii, 1978, **12**, 87.
59. L.A.Blyumenfel'd, V.V.Voevodskii, and A.G.Semenov, "Primenenie Elektronnogo Paramagnitnogo Rezonansa v Khimii" (Chemical Applications of Electron Paramagnetic Resonance), Izd.Nauka, Novosibirsk, 1962.
60. A.D.Milov, K.M.Salikhov, and M.D.Shchirov, Fiz. Tverd.Tela, 1981, **23**, 975.
61. M.Emshwiller, E.L.Hahn, and D.Kaplan, Phys.Rev., 1960, **118**, 414.
62. M.Huisyen and J.S.Hyde, Rev.Sci.Inst., 1974, **45**, 669.
63. B.N.Shelimov, N.N.Bubnov, N.V.Fok, and V.V.Voevodskii, Dokl.Akad.Nauk SSSR, 1960, **134**, 145.
64. N.M.Bazhin, Kinetika i Kataliz, 1967, **8**, 532.

Institute of Chemical Kinetics and Combustion, Siberian Division of the USSR Academy of Sciences, Novosibirsk